

SUPPLEMENTARY INFORMATION

METHODS

Molecular Docking Studies

The targeted pocket within the linker region was roughly defined by residues Asp212, Glu298, Glu301, Lys302, Asn303, Lys304, Phe312, Tyr315, Met337, Asn338, Lys353, Lys359, Asp361, Lys502 and Gln542. Although compounds in the Hitfinder library had been pre-screened for Lipinski rules (1), they were additionally treated with LigPrep v 1.6 res to generate lowest energy conformations, tautomers, and 3-dimensional versions of the chemicals(2). Ligands were docked using Glide SP, and the results were reported as a “Glide score” (3). A large grid was generated with outer box dimensions set to approximately 20 Å to include all possible regions within the pocket for potential inhibitor binding. QikProp v 2.3 was used to screen compounds for predicted ADME properties (4).

Inhibitor Assays

The RJF compounds were dissolved in DMSO. Enzyme concentration was determined spectrophotometrically by measuring absorbance at 280 nm with a molar extinction coefficient of 83740 M⁻¹ cm⁻¹ for the *P. falciparum* TS-DHFR enzyme and 25440 M⁻¹ cm⁻¹ for the *H. sapiens* DHFR enzyme. Briefly, DHFR steady-state activity was assessed by reacting enzyme with H₂-folate and NADPH, and following absorbance at 340 nm, which decreases as NADPH is depleted to form NADP⁺. An extinction coefficient of 12.8 mM⁻¹ cm⁻¹ was used for the DHFR reaction. TS steady-state activity was assayed by incubating the enzyme with CH₂H₄-folate and dUMP and following the increase in absorbance at 340 nm with the production of dTMP and H₄-folate. An

extinction coefficient of $6.4 \text{ mM}^{-1} \text{ cm}^{-1}$ was used for the TS reaction (5). An IC_{50} was determined by plotting rate versus inhibitor concentration and determining the inhibitor concentration at half maximal velocity (v_{max}). The rapid chemical quench assays were also performed under steady-state conditions to confirm patterns of inhibition shown by the spectrophotometric assay. A Kintek RFQ-3 rapid chemical quench instrument (Austin, TX) was used to perform the steady-state assays with radiolabeled substrates. The enzyme solution consisted of 0.75 - 1 μM enzyme in 2x reaction buffer (1 mM EDTA, 50 mM MgCl_2 , 50 mM Tris pH 7.8, saturating NADPH and dUMP either compounds dissolved in DMSO, or DMSO alone as control). The substrate solution consisted of 15 μM of 100 μM tritiated CH_2H_4 -folate, and the reaction was quenched with 67 μL of 0.78N KOH to a final concentration 0.54 μM . For the DHFR reaction, the enzyme solution consisted of 1 μM enzyme in 2x reaction buffer (1 mM EDTA, 50 mM MgCl_2 , 50 mM Tris pH 7.8, saturating NADPH and either compounds dissolved in DMSO, or DMSO alone as control). The substrate solution consisted of 15 μM of 100 μM tritiated H_2 -folate, and the reaction was quenched with 67 μL of 0.78N KOH to a final concentration 0.54 μM . The products were resolved using high performance liquid chromatography (HPLC) analysis. Detailed methods for the rapid chemical quench assays with tritiated substrates have been previously published (6).

Approximate relative free energy of binding to determine the preferred binding site

The following approximation of the free energy of binding (ΔG_{bind}) was utilized:

$$\Delta G_{\text{bind}} = \Delta E_{\text{int ra}} + \Delta G_{\text{solv}} + T\Delta S_{\text{conf}} + E_{\text{VDW}} + E_{\text{Elect}} + E_{\text{PTN}}$$

where ΔE_{intra} and ΔE_{solv} are intramolecular and desolvation penalties for each ligand upon binding, calculated by the difference between these quantities in the bound and unbound states; $T\Delta S_{conf}$ is the conformational entropy penalty of the ligand, which loses entropy upon binding; E_{PTN} is the intramolecular energy of the receptor which usually accounts for the deformation imposed by a ligand; E_{VDW} and E_{Elect} are intermolecular energies derived from the protein-ligand complexes.

To approximate interaction energies of the bound complexes, intramolecular and desolvation components were estimated using the OPLS_2005 force field and a Generalized Born implicit water model as implemented in Schrödinger's MacroModel (MacroModel, version 9.5, Schrödinger, LLC, New York, NY 2005) for structures produced from Glide. Each compound was first minimized in the complex while all other atoms were kept fixed, and a conformational search using the Monte Carlo Multiple Minimum method in MacroModel was performed on each of the four unbound ligands. The protein and cofactors used in docking were kept fixed to minimize noise in the protein intramolecular energy. This energy, as well as conformational entropy of the ligand, thus is constant for both the linker site and the active site.

$$\approx \Delta\Delta G_{bind} = (\Delta E_{intra} + \Delta G_{solv} + E_{VDW} + E_{Elect})_{SiteA} - (\Delta E_{intra} + \Delta G_{solv} + E_{VDW} + E_{Elect})_{SiteB}$$

Cell Culture Assays of Inhibitor Activity

The RJF compounds were dissolved in DMSO and tested in erythrocytic stages of both *P. falciparum* parasite with WT DHFR (TM4/8.2, a generous gift from S. Thaithong, Department of Biology, Faculty of Science, Chulalongkorn University), as well as the *P. falciparum* parasite with the N51I/C59R/S108N/I164L quadruple mutant of

DHFR (V1/S, from D. Kyle, through MR4). Detailed methods for cell culture assays of inhibitor activity were as previously described (7, 8).

Co-crystallization Studies and Data Analysis

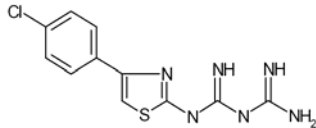
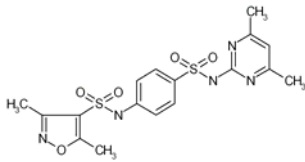
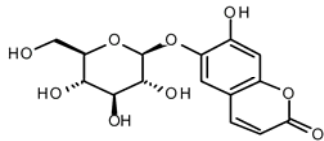
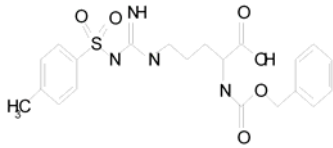
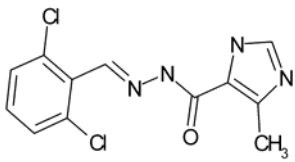
Each of purified enzymes (~15 mg/mL, ~0.16 mM) was crystallized in the presence of NADPH, dUMP, and either RJF 01302 or RJF 00670 (7.63 mM each) using the microbatch technique. Small prism crystals of both complexes were grown in similar conditions. RJF00670 complexed with the quadruple mutant TS-DHFR enzyme grew in 0.1 mM sodium acetate pH4.6, 15% (w/v) PEG4000, and 0.16M ammonium acetate. RJF01302 complexed with the WT TS-DHFR enzyme grew in 0.20M ammonium acetate, with all other conditions the same as the latter. For crystals with cycloguanil and the RJF compounds, the WT TS-DHFR enzyme was first co-crystallized first with 0.76 mM cycloguanil. The crystal was then soaked with the corresponding RJF compound for 72 h by adding 2.5 mM of either RJF 01302 and RJF 00670 or 1.25 mM of RJF 00719 into the well.

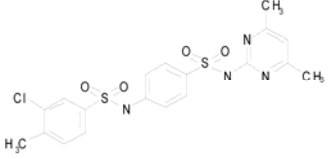
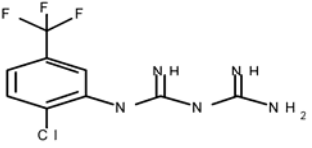
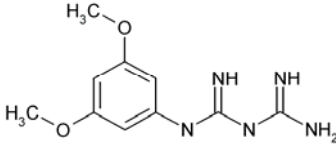
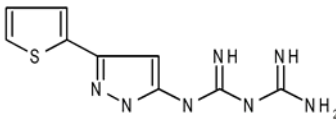
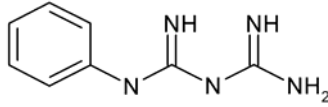
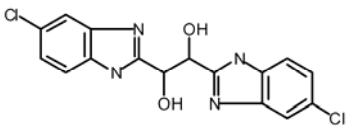
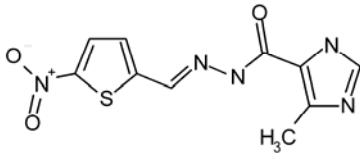
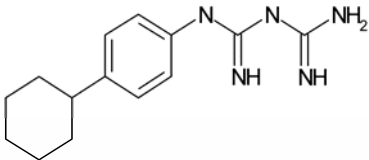
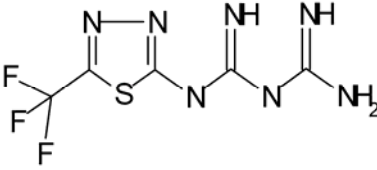
A single crystal of either WT or quadruple mutant was harvested into corresponding crystallizing solution containing 20% (v/v) glycerol as a cryoprotectant briefly before flash-frozen in liquid nitrogen. Data for quadruple mutant V1/S in complex with RJF670 were collected at beamline BL13B1 at the National Synchrotron Radiation Research Center (NSRRC, Taiwan) and processed using DENZO/SCALEPACK(9). Data for WT enzyme in complex with RJF01302 were measured using a Nonius FR591 rotating anode and Nonius CCD detector system. The structures were refined using CNS (10) combined with graphics inspection, as well as

model building and map fitting with O (11). PROCHECK (12, 13) in the CCP4 suite (14) was used for structure analysis, and images were prepared using Pymol (15). Otherwise, methods for co-crystallization of compounds with *P. falciparum* TS-DHFR and data analysis were as previously published (16). Protein-ligand interactions were determined using LigPlot v 4.4 (17).

TABLES

Supplementary Table 1. Glide SP docking results, and chemical structures, of top ‘hits’ for screening the Maybridge Hitfinder™ library against a non-active site pocket of WT *P. falciparum* TS-DHFR.

Rank	Maybridge Identifier Number	Glide Score	Chemical Structure
1	RJF 00587	-9.32	
2	HTS 07260	-9.30	
3	RJC 00925	-9.27	
4	BTB 13329	-9.22	
5	SPB 01617	-9.11	

6	HTS 07256	-8.94	
7	RJF 01302	-8.89	
8	RJF 00670	-8.87	
9	RJF 00729	-8.87	
10	RJF 01059	-8.66	
11	SPB 07799	-8.65	
12	SPB 01619	-8.61	
13	RJF 00719	-8.59	
14	RJF 00600	-8.50	

Supplementary Table 2. Predicted ADME Properties of Top ‘Hits’ of Glide Screen.

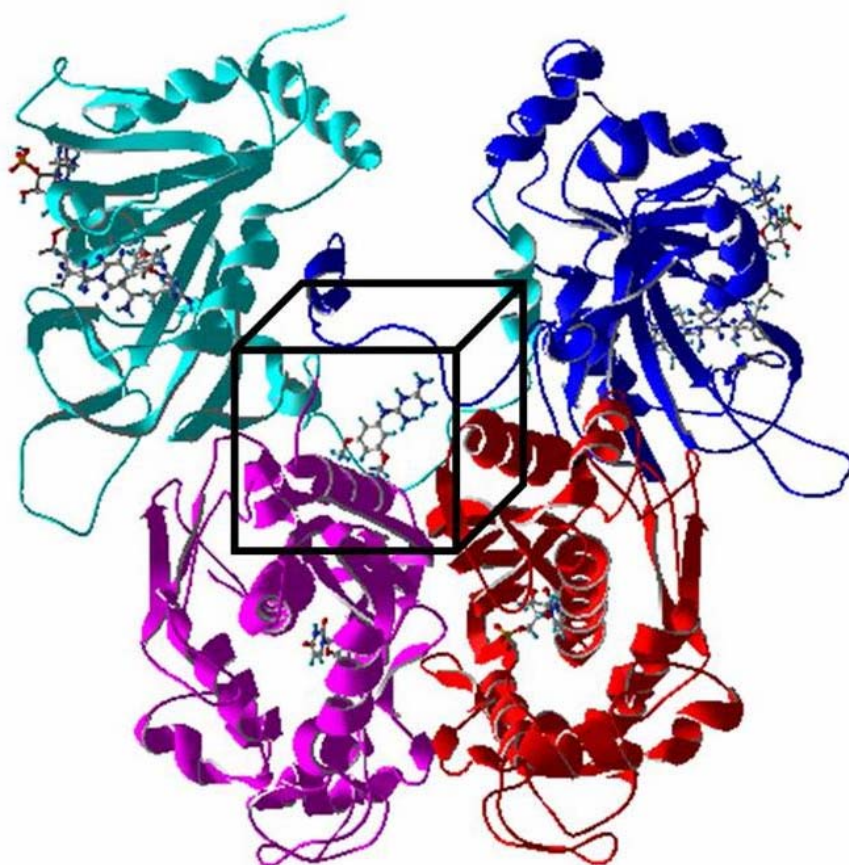
Maybridge Identifier	MW ^a	QP logP ^b	QP logS ^c	QP Caco ^d
----------------------	-----------------	----------------------	----------------------	----------------------

RJF 00587	296.8	1.0	-2.5	175
HTS 07260	435.5	-0.5	-1.5	72
RJC 00925	340.3	-1.6	-1.9	22
BTB 13329	462.5	1.7	-5.0	37
SPB 01617	298.2	3.9	-5.1	1021
HTS 07256	464.9	1.2	-3.2	142
RJF 01302	281.7	1.0	-1.8	213
RJF 00670	239.3	0.0	-0.9	174
RJF 00729	251.3	-0.4	-1.1	50
RJF 01059	179.2	-0.4	0.1	190
SPB 07799	364.2	2.7	-4.7	432
SPB 01619	280.3	2.2	-4.1	97
RJF 00719	261.4	0.9	-1.6	194
RJF 00600	255.2	-0.5	-1.4	67

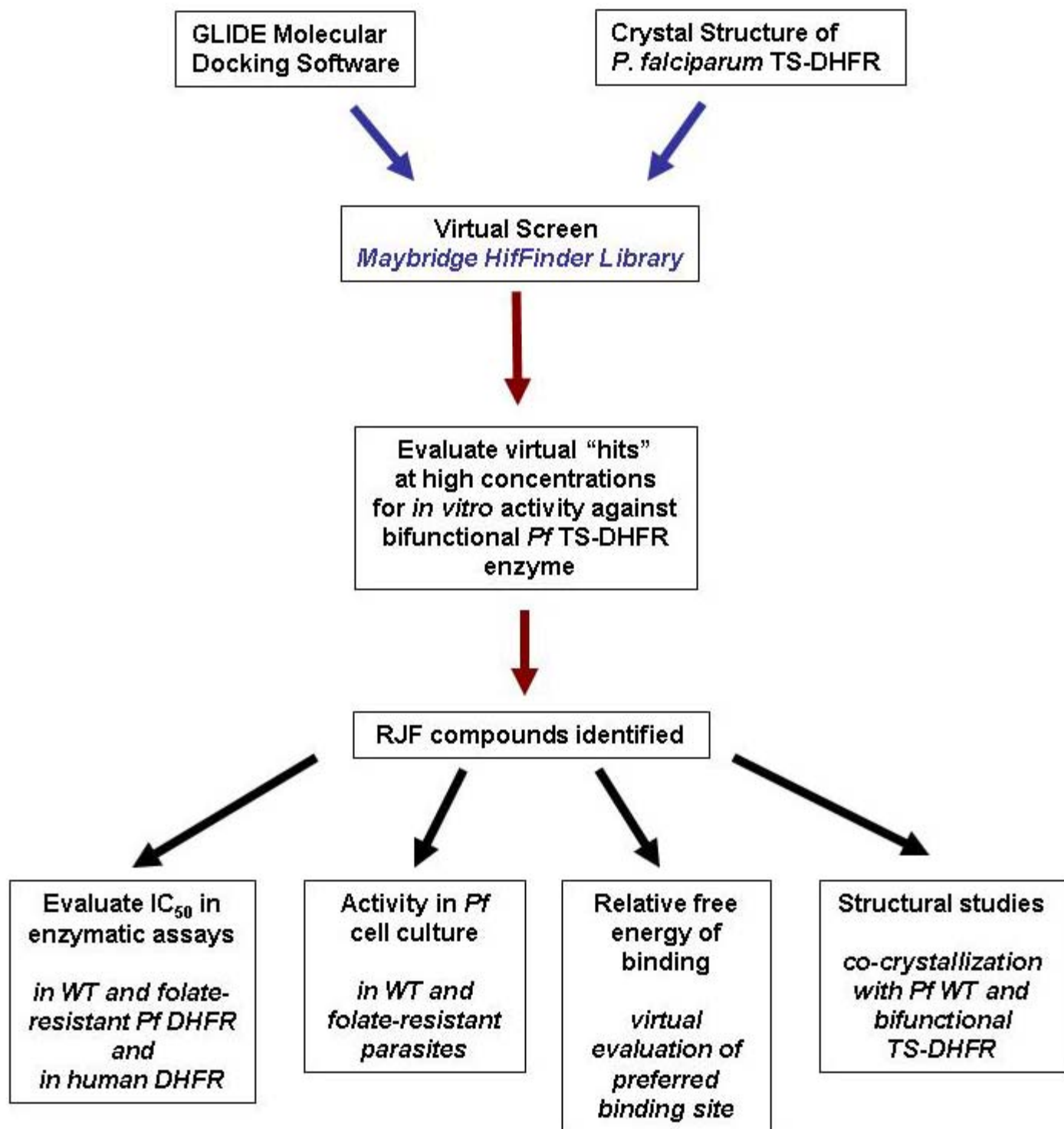
Supplementary Table 3. Hydrogen bond and hydrophobic interactions formed between *P. falciparum* DHFR active site and the inhibitors RJF 01302, RJF 00670, WR99210 and pyrimethamine. These interactions were calculated using LigPlot v 4.4 based on the crystal structures of these enzymes.

<i>Inhibitor</i>	<i>DHFR residues with which there are interactions</i>
RJF 00670	Ile 14, Cys 15, Ala 16, Asp 54, Phe 58, Leu 46, Met 104, Ile 112, Leu 119, Leu 164, Tyr 170
RJF 01302	Asp 54, Met 55, Phe 58, Ile 164
WR99210	Ile 14, Cys 15, Asp 54, Met 55, Phe 58, Ile 112, Pro 113, Leu 164
pyrimethamine	Ile 14, Cys 15, Ala 16, Asp 54, Phe 58, Asn 108, Ile 112, Ile 164, Tyr 170

Supplementary Figure 1. The crystal structure of *P. falciparum* TS-DHFR was used for molecular docking studies, with the black 20Å box representing the boundary conditions for the Glide docking calculations. DHFR domains are shown in dark and light blue, and TS domains are shown in pink and red. RJF 00670 is shown at the center of the box. This figure is adapted from reference Lyons, T.M. (2006) (18).

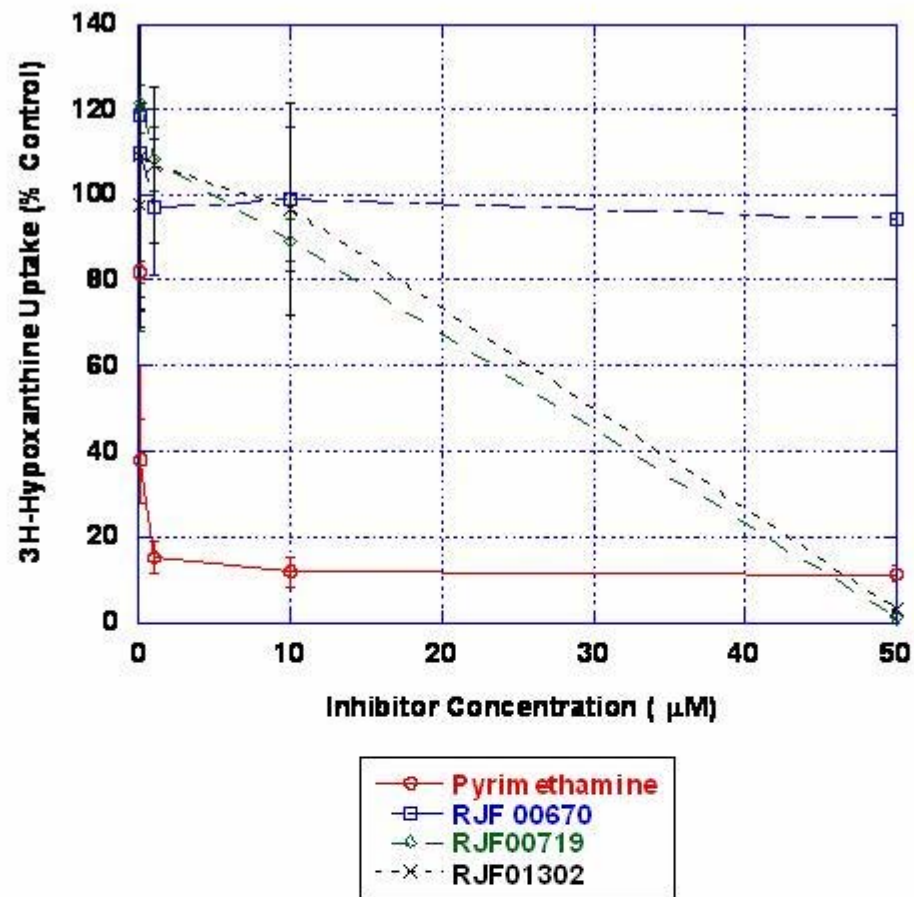


Supplementary Figure 2. Flow diagram of virtual screening and lead compound identification.

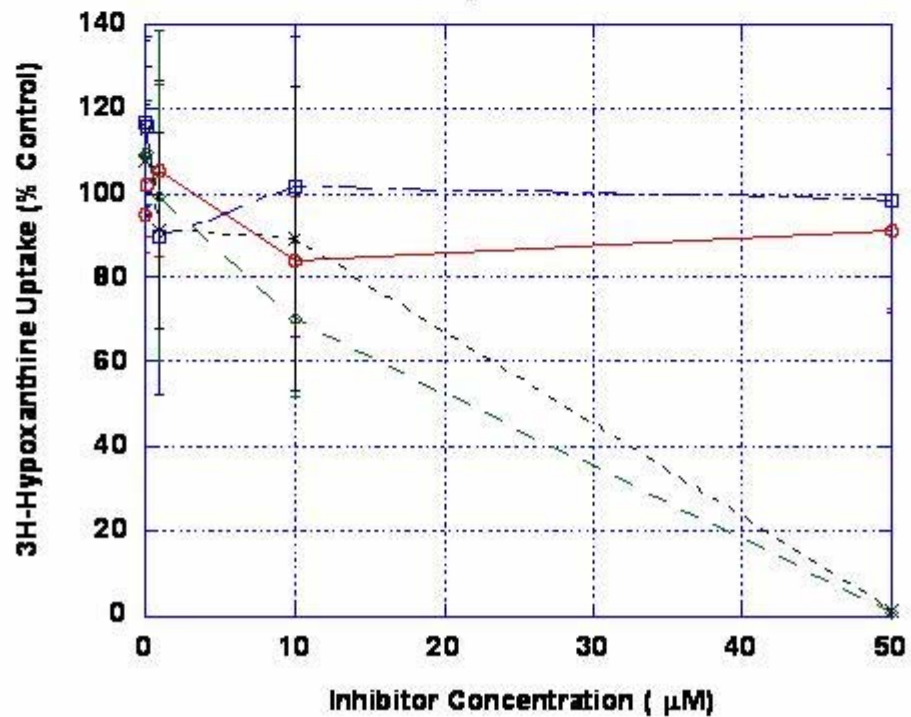


Supplementary Figure 3. IC₅₀ curves for RJF 00670, RJF 01302 and RJF 00719 with *P. falciparum* WT and quadruple mutant DHFR.

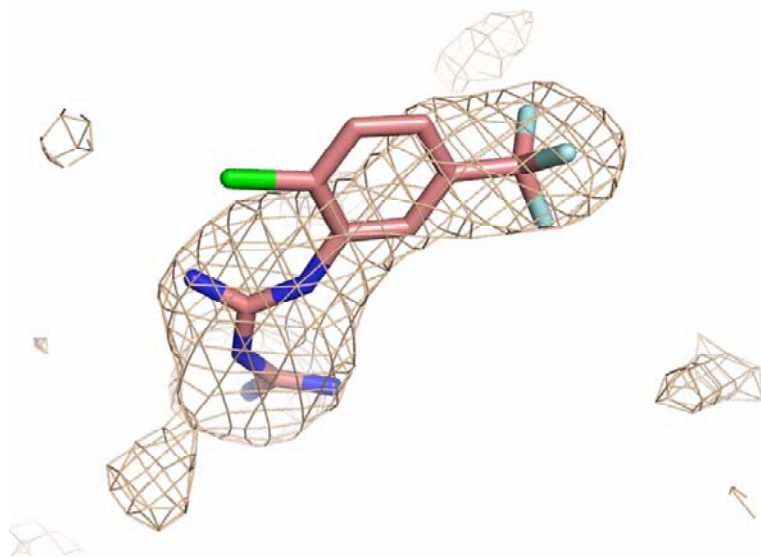
WT



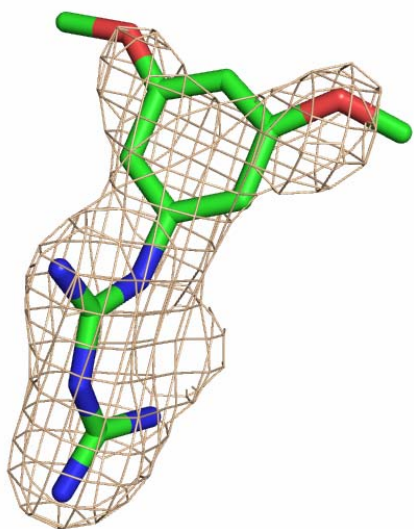
Quadruple Mutant



Supplementary Figure 4. Fo-Fc Map for RJF01302 in complex with WT TS-DHFR enzyme



Supplementary Figure 5. Fo-Fc Map for RJF00670 in complex with quadruple mutant TS-DHFR enzyme



REFERENCES

- (1) Lipinski, C. A., Lombardo, F., Dominy, B. W., and Feeney, P. J. (2001) Experimental and computational approaches to estimate solubility and

- permeability in drug discovery and development settings. *Adv Drug Deliv Rev* 46, 3-26.
- (2) *Ligprep v 1.6*, Schrodinger, LLC, New York.
 - (3) *Glide v 3.5*, Schrodinger, LLC, New York.
 - (4) Jorgensen, W. L., and Duffy, E. M. (2002) Prediction of drug solubility from structure. *Adv Drug Deliv Rev* 54, 355-66.
 - (5) Meek, T. D., Garvey, E. P., and Santi, D. V. (1985) Purification and characterization of the bifunctional thymidylate synthetase-dihydrofolate reductase from methotrexate-resistant *Leishmania tropica*. *Biochemistry* 24, 678-86.
 - (6) Dasgupta, T., and Anderson, K. S. (2008) Probing the Role of Parasite-Specific, Distant Structural Regions on Communication and Catalysis in the Bifunctional Thymidylate Synthase-Dihydrofolate Reductase from *Plasmodium falciparum*. *Biochemistry* 47, 1336-45.
 - (7) Kamchonwongpaisan, S., Quarrell, R., Charoensetakul, N., Ponsinet, R., Vilaivan, T., Vanichtanankul, J., Tarnchompoo, B., Sirawaraporn, W., Lowe, G., and Yuthavong, Y. (2004) Inhibitors of multiple mutants of *Plasmodium falciparum* dihydrofolate reductase and their antimalarial activities. *J Med Chem* 47, 673-80.
 - (8) Ponmee, N., Chuchue, T., Wilairat, P., Yuthavong, Y., and Kamchonwongpaisan, S. (2007) Artemisinin effectiveness in erythrocytes is reduced by heme and heme-containing proteins. *Biochem Pharmacol* 74, 153-60.
 - (9) Otwinowski, Z., and Minor, W. (1997) in *Processing of X-ray diffraction data collected in oscillation mode*. pp 307-326, Academic press, New York.
 - (10) Brunger, A. T., Adams, P. D., Clore, G. M., DeLano, W. L., Gros, P., Grosse-Kunstleve, R. W., Jiang, J. S., Kuszewski, J., Nilges, M., Pannu, N. S., Read, R. J., Rice, L. M., Simonson, T., and Warren, G. L. (1998) Crystallography & NMR system: A new software suite for macromolecular structure determination. *Acta Crystallogr. D* 54 (Pt 5), 905-21.
 - (11) Jones, T. A., Zou, J. Y., Cowan, S. W., and Kjeldgaard, M. (1991) Improved methods for building protein models in electron density maps and the location of errors in these models. *Acta Crystallogr. A* 47, 110-119.
 - (12) Laskowski, R. A., MacArthur, M. W., Moss, D. S., and Thornton, J. M. (1993) PROCHECK: a program to check the stereochemical quality of protein structures. *J. Appl. Cryst.* 26, 283-291.
 - (13) Morris, A. L., MacArthur, M. W., Hutchinson, E. G., and Thornton, J. M. (1992) Stereochemical quality of protein structure coordinates. *Proteins* 12, 345-364.
 - (14) Project, C. C. (1994) The CCP4 Suite: Programs for Protein Crystallography. *Acta Crystallogr. D* 50, 760-763.
 - (15) DeLano, W. L. (2002) The PyMOL Molecular Graphics System, DeLano Scientific, San Carlos, CA, USA. .
 - (16) Chitnumsub, P., Yuvaniyama, J., Vanichtanankul, J., Kamchonwongpaisan, S., Walkinshaw, M. D., and Yuthavong, Y. (2004) Characterization, crystallization and preliminary X-ray analysis of bifunctional dihydrofolate reductase-thymidylate synthase from *Plasmodium falciparum*. *Acta Crystallogr D Biol Crystallogr* 60, 780-3.

- (17) Wallace, A. C., Laskowski, R. A., and Thornton, J. M. (1995) LIGPLOT: a program to generate schematic diagrams of protein-ligand interactions. *Protein Eng* 8, 127-34.
- (18) Lyons, T. M. (2006) in *Department of Chemistry* pp 121, Yale University, New Haven.